

# Testing the Zonal Stationarity of Spatial Point Processes: Applied to prostate tissues and trees locations

Azam Saadatjouy    and Ali Reza Taheriyoun\*    and Mohammad Q. Vahidi-Asl

**Abstract:** We consider the problem of testing the stationarity and isotropy of a spatial point pattern based on the concept of local spectra. Using a logarithmic transformation, the mechanism of the proposed test is approximately identical to a simple two factor analysis of variance procedure when the variance of residuals is known. This procedure is also used for testing the stationarity in neighborhood of a particular point of the window of observation. The same idea is used in post-hoc tests to cluster the point pattern into stationary and nonstationary sub-windows. The performance of the proposed method is examined via a simulation study and applied in a practical data.

**AMS 2000 subject classifications:** Primary 60G55, 62M15; secondary 62F15.

**Keywords and phrases:** complete covariance density function, evolutionary periodogram, spatial point process, spectral density function, zonal stationarity.

Received 22 January 2017.

## 1. Introduction

### 1.1. General aspects

A point pattern as a realization of a point process is a set of points that are distributed irregularly in a window. The analysis of a point pattern provides information on the geometrical structures formed by the aggregation and interaction between points. The aggregation and interaction of points are characterized by intensity and covariance density functions, respectively. The spectral density function of a stationary point process is the Fourier transform of the complete covariance density function and is estimated in an asymptotically unbiased manner by the spatial periodogram. For a stationary point process all the second-order characteristics (e.g., the complete covariance density function) are only a function of inter-points distances and thus the spectral density function does not depend on the locations of points. So, the structure of the complete covariance density and spectral density functions may vary with location when the stationarity assumption is violated.

---

\*Corresponding author

Several efficient methods based on the spectral density are available in the literature for studying the spatial structure of stationary processes. The spectral methods were used by [7] to investigate the asymptotic properties of several estimation procedures for a stationary process observed on a  $d$ -dimensional lattice. The approximated locations of events in a spatial point pattern were presented using the intersections of a fine lattice on the observation window by [19] and the point spectrum was approximated by the lattice spectrum.

Generally, a vague boundary exists between stationary and nonstationary point processes containing zonal stationary. The source of nonstationarity of these processes is the local regular behavior. These processes are further explained in Section 2.1. Based on a point pattern, we want to decide between the zonal stationarity and the simple stationarity assumption. One may suggest to employ the methods developed for regular observation of random fields. To this end, since the point pattern is an irregular observation of points, we need to partition the observation window,  $W$ , into a regular  $d$ -dimensional grid where the  $i$ th edge of  $W$  is divided into  $n_i$ ,  $i = 1, \dots, d$ , equidistant parts. Let  $N_{\mathbf{i}}$  represent the number of points in the sub-cube in the  $\mathbf{i}$ th row, where  $\mathbf{i} = (i_1, \dots, i_d)$ , and  $i_j = 1, \dots, n_j$ . We consider the  $N_{\mathbf{i}}$  as a measured variable at the  $\mathbf{i}$ th grid and evaluate the stationarity of the point pattern by testing the stationarity of  $\{N_{\mathbf{i}}\}_{\mathbf{i}}$  random field. This test is similar to the test for stationarity of random fields introduced by [6] which loses the information about the locations of points. In the second approach, we define the evolutionary spectra for the realization of a point process and then examine the local behavior of the discrete evolutionary spectra. The stationarity assumption is rejected if the spectral density function shows different behavior at least in two different regions of the window. We mention the property of different behaviors in different regions by *second-order location dependency*. Our method is designed to detect this behavior against the second-order stationarity.

The concept of evolutionary (i.e. time-dependent) spectra has been introduced by [16, 15]. Testing the stationarity of time series is a very famous consequences of this concept [18]. The asymptotic properties of nonstationary time series with locally stationary behavior was investigated by [4] using the time-dependent spectra. The remaining references somehow used the evolutionary or local spectra for testing the stationarity of regular trajectories of random fields except [1] which proposed a test for spatial stationarity based on a transformation of irregularly spaced spatial data. A nonparametric and several parametric procedures for modeling the spatial dependence structure of a nonstationary spatial process observed on a  $d$ -dimensional lattice was proposed by [5]. Priestley's idea was extended to test the stationarity and isotropy of a spatial process [6]. Fluctuations of the local variogram for testing the stationarity assumption of a random process was employed in [3]. A formal test for stationarity of spatial random fields on the bases of the asymptotic normality of certain covariance estimators at certain spatial lags was derived by [10]. A wavelet-based analysis of variance for a stationary random field on a regular lattice was used by [13] for testing the stationarity.

This paper is organized as follows: In the sequel, we study two motivating

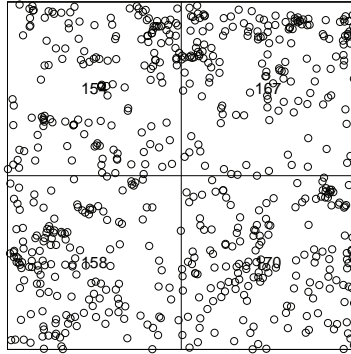


Fig 1: The locations of 649 trees of the Bar Colorado forest in a rectangular window whose vertices are located at the geographic coordinates  $(500, 0)$  and  $(700, 333/3333)$ . The sampling window is rescaled into  $[0, 70]^2$ .

datasets. in the following section, we review some concepts of point processes and present two spatial spectral representations for a nonstationary spatial point process. Moreover, the nonparametric estimates of the spectral density of a nonstationary point process are proposed in this section. A formal test of stationarity is presented in Section 3. In Section 4, we examine the proposed testing approaches via a simulation study. We also study the effect of location in the competition between a specific genus of trees in 4.1.

## 1.2. Data and motivations

In this section, we propose two datasets as well as motivations for data analysis in order to further illustrate the mentioned problem throughout this study. The first dataset is devoted to the location of *Euphorbiaceae* trees in a part of the Bar Colorado forest (Figure 1). Generally, one of the main and essential information for forest management and its optimal and sustainable utilization is to determine the frequencies of different types of trees, distribution pattern of trees, and their competition. For example, the distribution of trees seeds could have an impact on their aggregation while competition among different species for moisture, light, and nutrients acts vice versa. A positive autocorrelation or aggregation may result from regeneration near parents, whilst a negative autocorrelation results from their competition. Therefore, it seems that variations of the aggregation structure will be change the interaction structure of trees. Since the local periodogram is influenced by the aggregation and interactions of points, so we use this function for detecting the location(s) at which the structure of trees pattern is changed.

The second data is the location of capillary profiles on a section of prostate tissue. According to the anatomy of the human body, blood circulation in the human body starts from heart, then flows through arteries, and finally receives

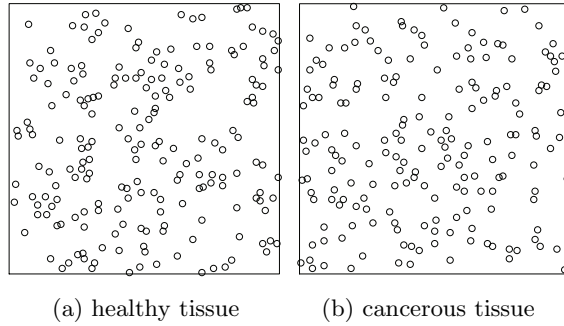


Fig 2: The locations of 196 capillaries on a section of a healthy prostate (2a) and the locations of 185 capillaries at the same section from a cancerous prostate (2b).

to all parts of the body by capillaries. Capillaries are the smallest vessels of the body, supplying the oxygen to tissues and exchanging constituents between tissues and blood. Figure 2 manifests the midpoints of the capillaries in sections of healthy and cancerous prostate tissues. The rescaled point patterns published by [8] were used to capture the coordinates of the capillaries. Since the quantity of nutrients and oxygen required by different parts of a given organ of the body are not same, so it is expected that the density of capillary network will be different in various parts of the body. In order to scrutinize this issue, we examine the behavior of evolutionary periodogram function at different parts of a tissue.

## 2. Nonstationary spectral approaches

### 2.1. Preliminaries

A point process is called stationary if its distribution is invariant under translations and is called isotropic if its distribution is invariant under rotations about the origin in  $\mathbb{R}^d$ . For a stationary point process the intensity function is constant and the second-order characteristics depend only on the lag vector. Moreover, for an isotropic process such dependency is an exclusive function of the scalar length of lag vector regardless of the orientation. Moving to the frequency domain approaches, the spectral density function of a point process is the Fourier transform of the complete covariance density function. It is a function like  $f_{XX} : \Omega \rightarrow \mathbb{C}$ , where  $\Omega$  is the space of frequencies and is defined as (see [14]) the Fourier transform of the unit-free complete covariance density function,  $\kappa_{XX}$  [2]. For a nonstationary spatial process, [6] generalized the concept of evolutionary spectra of time series introduced by [16]. Following the same idea, we introduce two different evolutionary periodograms of nonstationary point processes. A new class of nonstationary point processes called ‘zonal’ sta-

tionary processes is introduced. In each approach, an empirical spectral density function is defined for this class of nonstationary point process whose physical interpretation is similar to that of the spectrum of a stationary point process, but it is varying with location. Intuitively, a point process is called zonal stationary if it behaves in an approximately stationary way in a neighborhood of some point. In other words, a point process  $X$  is called zonal stationary on  $W$  if there exist finite points  $\mathbf{z} \in W$  such that for some  $\rho > 0$ ,  $X_{b(\mathbf{z}, \rho)}$  is stationary, where  $X_B$  denotes the restriction of  $X$  to  $B$  and  $b(\mathbf{z}, \rho)$  denotes a closed ball centered at  $\mathbf{z}$  with a radius  $\rho$ . Figure 3 shows a realization of zonal stationary point process in the window  $W = [0, 70]^2$ . We term  $z_1, \dots, z_9$  the middle points of  $\mathbf{S}_1, \dots, \mathbf{S}_9$  square sub-windows from left to right and down to up, respectively. In this figure, the point pattern in  $\mathbf{S}_3$  is a realization of the stationary Thomas process, in  $\mathbf{S}_8$  we have a realization of the Simple Sequential Inhibition (SSI) process and the remaining are realizations of stationary Poisson processes.

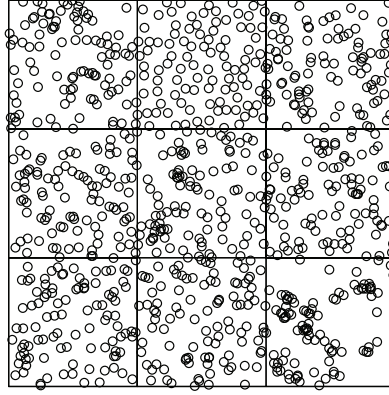


Fig 3: A realization of the zonal stationary point process.

The regional behavior of a point pattern can be detected through evaluating its different features in the special regions. For this aim, closed balls with centers at different points of the observation window are typically considered in the spatial domain. Moreover, the local behavior of the point pattern is decided on the basis of measuring its different features at these balls. However, determining these regions and different features are crucial in the spatial domain. Fortunately, this issue can be easily solved in the frequency domain. This could be attributed to the fact that the frequency domain is based on  $[-\pi, \pi]$  regardless of the form of the observation window. The Bartlett window can be used to determine different regions on which the features must be evaluated and accordingly the regional behavior of the point pattern can be detected by computing the local periodogram.

Suppose that we have a point process  $X$  observed on a rectangular window  $W = [\mathbf{0}, \mathbf{l}]$ , where  $\mathbf{l} = (l_1, \dots, l_d)$ , that is the rectangular window with a vertex at the origin of the Cartesian coordinates and an opposite vertex on  $\mathbf{l}$ . Construct

$\{N_{\mathbf{i}}\}_{\mathbf{i}}$  as before. We consider a regular  $n_1 \times \dots \times n_d$  grid on the study area and set  $n = \prod_{j=1}^d n_j$ . Let  $N_{\mathbf{i}}$  be the number of points in the  $\mathbf{i}$ th row where  $\mathbf{i} = (i_1, \dots, i_d)$  and  $i_j = 1, \dots, n_j$  for  $j = 1, \dots, d$ . We consider the  $N_{\mathbf{i}}$  as a measured variable at the  $\mathbf{i}$ th quadrant and define the random field as  $V(\mathbf{s}) = N_{\mathbf{i}}$  if  $\mathbf{s}$  belongs to the  $\mathbf{i}$ th row. Figure 4 shows the image of  $N_{\mathbf{i}}$  random field obtained by considering a  $70 \times 70$  regular grid on  $y$ . Now, one may use the method of [6] to define the

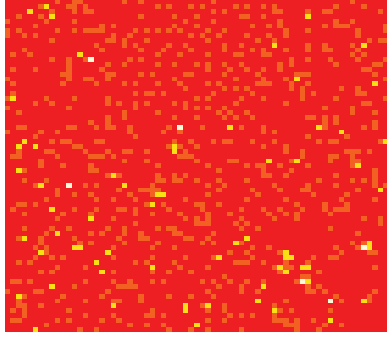


Fig 4: The regular realization of the  $N_{\mathbf{i}}$  random field corresponding to the mentioned point pattern in Figure 3.

local periodogram of the obtained random field which eliminate the information about the locations. Our approach is the nonstationary periodogram.

## 2.2. Nonstationary periodogram of point processes

Assume that we have a point pattern  $x$  observed on a rectangular window  $W = [0, 1]$  containing  $n_X$  points. Let  $D = \{\mathbf{u}_j = (u_{1j}, \dots, u_{dj}), j = 1, \dots, n_X\}$ , be the set of positions of the points. Suppose the approximate locations of points in a point pattern be represented by the intersections of a  $m_1 \times \dots \times m_d$  fine lattice superimposed on the study region. This lattice generates an irregular realization of a binary random field. We define the obtained realization,  $\zeta$  say, from the random field  $\zeta$  as

$$\zeta(\mathbf{s}) = \begin{cases} 1 & \text{if } \mathbf{s} \in D \\ 0 & \text{if } \mathbf{s} \notin D. \end{cases}$$

$\zeta(\mathbf{s})$  is a simple random field and only the positions at which events occur are of interest. There is an equivalence between the point spectra of  $X$  and the spectra of the random field  $\zeta$  [19]. If  $X$  is a stationary point process, then  $\zeta$  will be a stationary random field. Consequently, any evidence of nonstationarity of  $\zeta$  could be a reason for rejection of the stationarity hypothesis of  $X$ . Suppose that  $\zeta$  be zonal stationary, then its spectral density function, denoted by  $f_z(\omega)$ , is the Fourier transform of the locally auto covariance function of  $\zeta$  and  $z$  is

the location around that  $\zeta$  behaves in a stationary manner (see [6]). If for a given  $z$  the function  $f_z(\omega)$  is not sensitive to  $\omega$ , then we conclude that in the neighborhood of the given  $z$ ,  $f_z(\omega)$  belongs to a completely spatial random point pattern. On the other hand, if for a given frequency  $\omega$ ,  $f_z(\omega)$  is not sensitive to  $z$ , then we conclude that for the given  $\omega$ ,  $f_z(\omega)$  dose not behave locally. Practically,  $f_z(\omega)$  is unknown for every  $z$  and for every  $\omega$  and we restrict the problem of estimation to specific Fourier frequencies and locations. Therefore, our approach is a parametric statistical inference.

Consider a location varying filter to assign greater weights to the neighboring values of  $z$ . The spatial local periodogram at a location  $z$  and frequency  $\omega$  is  $|\mathcal{J}_z(\omega)|^2$ , where

$$\begin{aligned}\mathcal{J}_z(\omega) &= \frac{1}{\sqrt{\prod_{j=1}^d l_j}} \sum_{k=1}^m g(z - \mathbf{s}_k) \zeta(\mathbf{s}_k) \exp\{-i\mathbf{s}_k^T \omega\} \\ &= \frac{1}{\sqrt{\prod_{j=1}^d l_j}} \sum_{j=1}^{n_x} g(z - \mathbf{u}_j) \exp\{-i\mathbf{u}_j^T \omega\} \\ &= A_z(\omega) + iB_z(\omega),\end{aligned}\tag{1}$$

where  $g : \mathbb{R}^d \rightarrow \mathbb{R}$  is the filter function with all the characteristics mentioned by [6] with finite width  $B_g$  defined as  $B_g = \int_{\mathbb{R}^d} |\mathbf{u}| |g(\mathbf{u})| d\mathbf{u}$ , and  $m = m_1 \times \dots \times m_d$ . The resulting periodogram is not smooth enough to be used as an estimation of the local spectra and thus  $|\mathcal{J}_z|^2$  is smoothed using the  $\mathbb{L}^2$  kernel family,  $\{W_\rho\}$ , where for each  $\rho$  there exists a constant  $C$  such that

$$\lim_{\rho \rightarrow \infty} \rho^d \int_{\mathbb{R}^d} |w_\rho(\lambda)|^2 d\lambda = C,\tag{2}$$

where  $w_\rho$  is the Fourier transform of  $W_\rho$ . Thus, the final estimator is

$$\hat{f}_z(\omega) = I_z(\omega) = \int_{\mathbb{R}^d} W_\rho(z - \mathbf{u}) |\mathcal{J}_z(\omega)|^2 d\mathbf{u}.\tag{3}$$

Using the very similar arguments employed by [6], the covariance between the spatial periodogram values  $I_{z_1}(\omega)$  and  $I_{z_2}(\omega')$  will be asymptotically zero if either  $\|\omega \pm \omega'\| \gg \text{bandwidth of } |\Gamma(\theta)|^2$  where  $\Gamma$  is the Fourier transform of  $g$  and or  $\|z_1 \pm z_2\| \gg \text{bandwidth of the function } W_\rho(\mathbf{u})$  [17]. For fixed  $z$  and  $\omega$ , one may conclude the normality of  $A_z(\omega)$  and  $B_z(\omega)$  similar to the [14].

Figure 5 shows the spatial local periodogram of the mentioned  $y$  in Figure 4 at the locations  $z_1, \dots, z_9$  which are enough wide apart and at the Fourier frequencies. The number of observed points of  $y$  in the considered sub-windows are almost similar. Obviously, as shown in Figure 5, the behavior of the local periodogram function of  $y$  varies at different locations. The shape of the local periodograms in sub-windows with stationary Poisson patterns (around  $z_k$ ,  $k \in K = \{1, 2, 4, 5, 6, 7, 9\}$ ), are broadly flat, reflecting the absence of the interaction structure in the observed patterns. In the sub-window with the stationary Thomas pattern, for small values of  $\|\omega\|$  the values of  $I_{z_3}(\omega)$  are larger in comparison with  $I_{z_j}(\omega)$  when  $j \in K$ . In contrast, the sub-window with the Simple Sequential Inhibition pattern, the values of  $I_{z_8}(\omega)$  are smaller than  $I_{z_j}(\omega)$ ,  $j \in K$ , for small  $\|\omega\|$ .

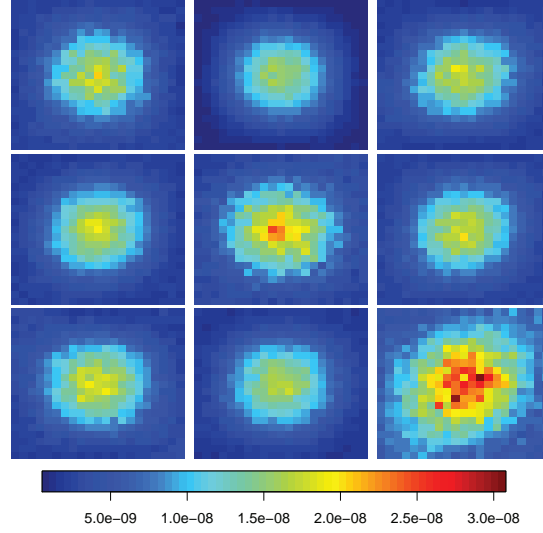


Fig 5: The spatial local periodogram of the point pattern of Figure 3 at the locations  $z_1, \dots, z_9$  and Fourier frequencies

There is a fundamental difference between this location dependent point spectra and the lattice-based local spectra considered by [6]. A lattice-based spectrum describes the spatial structure of a measured variable (for example, tree heights) at fixed equally spaced locations in an  $n_1 \times n_2$  grid. However, in a local point spectrum, we consider the spatial structure of the location (for example, locations of trees) of points instead of a measured characteristic. Moreover, the first estimator ignores the information about the precise locations of points compared with the second one.

Concerning the Bartlett's window,  $g(\mathbf{u})$  is considered as a multiplicative filter in the simulation study of Section 4; i.e.  $g(\mathbf{u}) = \prod_{j=1}^d g_1(u_j)$ , where  $g_1(u) = (4\pi h)^{-1/2} \mathbf{1}_{|u| \leq h}$ . Thus the Fourier transform of  $g$  becomes  $\Gamma(\boldsymbol{\omega}) = \prod_{j=1}^d (\sqrt{h\pi}\omega_j)^{-1} \sin(h\omega_j)$ . Further, we consider  $W_\rho(\mathbf{u})$  to be of the form  $W_\rho(\mathbf{u}) = \prod_{j=1}^d W_{1,\rho}(u_j)$ , where  $W_{1,\rho}(u) = 1/\rho \mathbf{1}_{|u| \leq \rho/2}$ , corresponding to the Daniell window which implies the accuracy of formula (2) with  $C = (2\pi)^d$ .

### 3. Testing the stationarity

In this section, we represent a formal test of stationarity of a point process based on the results discussed in the previous section. The analysis of the geometric structure of a point pattern is strongly related to the aggregation of points and interaction between points. When the aggregation of points is the same at two different sub-windows it is not easy to visually discriminate the interaction effect



in these sub-windows. In this situation, the higher moments of the point pattern such as the second order intensity function must be compared together in different areas. If the restricted point patterns to disjoint sub-windows are assumed to be independent, their second order properties can be compared according to [20]. Without such independence, the *two-factor analysis of variance* model and the assumptions considered in the following are valid. We thus write (see also [9, 18])

$$Y(z, \omega) = \ln I_z(\omega) = \ln f_z(\omega) + \varepsilon(z, \omega). \quad (4)$$

[18] showed that for  $\omega \in \prod_{j=1}^d [-\pi/\Delta_j, \pi/\Delta_j]$ , the asymptotic mean and variance of  $\varepsilon$  are  $\mathbb{E}(\varepsilon(z, \omega)) = 0$  and

$$\sigma^2 = (C/\rho^d) \int_{\mathbb{R}^d} |\Gamma(\theta)|^4 d\theta, \quad (5)$$

which is independent of  $z$  and  $\omega$ .

We select a set of locations  $z_1, z_2, \dots, z_m$  and a set of frequencies  $\omega_1, \omega_2, \dots, \omega_n$  in such a way that an acceptable sample is gathered in location and frequency spaces and we evaluate  $I_z(\omega)$  over this fine sample. The set of locations and frequencies must also be wide apart enough in order to  $\varepsilon(z_i, \omega_j)$  and consequently  $I_{z_i}(\omega_j)$  be uncorrelated. If we write  $Y_{ij} = Y(z_i, \omega_j)$ ,  $f_{ij} = \ln f_{z_i}(\omega_j)$  and  $\varepsilon_{ij} = \varepsilon(z_i, \omega_j)$ , then using the discussion on the normality of  $A_z$  and  $B_z$ , the noise terms,  $\varepsilon_{ij}$ , are considered to be normally distributed and  $Y_{ij}$  are generated according to the model

$$Y_{ij} = f_{ij} + \varepsilon_{ij}.$$

The parameter  $f_{ij}$  represents the treatment effect for location effect at level  $z_i$  and the frequency effect at level  $\omega_j$ . By considering the normality of the main effects, we can rewrite the model as

$$H_1 : Y_{ij} = \mu + \alpha_i + \beta_j + \gamma_{ij} + \varepsilon_{ij}, i = 1, \dots, m \quad \text{and} \quad j = 1, \dots, n. \quad (6)$$

In this model, the parameters  $\alpha_i$  and  $\beta_j$  represent the main effects of the location and frequency factors, respectively, and  $\gamma_{ij}$  represents the interaction between these two factors. As previously mentioned, the spectral density function of a stationary point process does not oscillate locally and it only varies by change of the frequencies. Therefore, the stationarity of a point process can be tested by using the analysis of variance methods and testing the model

$$H_0 : Y_{ij} = \mu + \beta_j + \varepsilon_{ij}, i = 1, \dots, m \quad \text{and} \quad j = 1, \dots, n,$$

or equivalently  $H_0 : \alpha_i = 0, i = 1, \dots, m$ , versus (6). The rejection of  $H_0$  represents that at least one of the parameters  $\alpha_i$  is not zero which means that there exists at least one  $z_i \in W$  in such a way that  $f_{z_i}(\omega) \neq f_{z_j}(\omega)$  for all  $j \neq i$ . A post-hoc test is used to find the different location(s) and thus we may use this as a clustering method in zonal stationary point processes. Since the value of

$\sigma^2 = \text{Var}(\varepsilon_{ij})$  is known, the presence of the interaction factor,  $\gamma_{ij}$ , can be tested only using one realization of the point process. If the effect of interaction factor is not significant, then the point process is uniformly modulated and  $\ln f_z(\omega)$  will be additive in terms of location and frequency. We can examine whether the nonstationarity of the point pattern is restricted only to some frequencies, by selecting those frequencies and testing for stationarity over them. If  $X$  is an isotropic point process, then  $f_z(\omega)$  depends on its vector argument  $\omega$  only through its scalar length  $\|\omega\|$ , regardless of the orientation of  $\omega$ . Then, we can test for isotropy by selecting a set of frequencies with the same norms, say  $\{\omega_{j_1}, \omega_{j_2}\}$  where  $\omega_{j_1} \neq \omega_{j_2}$  but  $\|\omega_{j_1}\| = \|\omega_{j_2}\|$ , and test whether the frequency effect is significant. Since  $\sigma^2$  is known, all of these comparisons are based on a  $\chi^2$  rather than  $F$ -test.

#### 4. Simulation study

In this section, we evaluate the performance of the proposed test for detecting the nonstationarity of a point process. As mentioned in the previous section, using a logarithmic transformation, the mechanism of the test are almost identical to those of a two-factor analysis of variance procedure.

In testing for stationarity, firstly we consider the interaction sum of squares. If the interaction is not significant, we conclude that the point process is a uniformly modulated process and continue to test for stationarity by evaluating the ‘between spatial locations’ sum of squares. If the interaction sum of squares turns out to be significant, we conclude that the point pattern is nonuniformly modulated and nonstationary. In this situation, we can survey whether the nonstationarity of the point process is restricted only at some frequencies. Significance of the ‘between spatial locations’ sum of squares means that the point pattern is nonstationary.

We set the nominal level of test at 0.05 and assume that all of the point processes are observed on a rectangular window  $W = [0, 70]^2$ . Using (1), for all cases, we estimate  $f_z(\omega)$  in which  $g(\mathbf{u})$  and  $W_\rho(\mathbf{u})$  employ  $h = 3$  and  $\rho = 20$ , respectively. The bandwidth of  $|\Gamma(\omega_1)|^2$  is approximately  $\pi/h = \pi/3$ . The window  $W_\rho(\mathbf{u})$  has a bandwidth of  $\rho = 20$ . Thus, the space between  $z_i$  and  $\omega_j$  points must be at least  $\rho = 20$  and  $\pi/3$  respectively, in order to obtain approximately uncorrelated estimates. The points  $z_i$  are chosen as  $z_i = (z_{i_1}, z_{i_2}) = (70i_1/6, 70i_2/6)$  with  $i_1 = 1(2)5$  and  $i_2 = 1(2)5$ , corresponding to a uniform spacing of  $70/3$  (just exceeding  $\rho = 20$ ). The frequencies are chosen as  $\omega_1 = (\pi/20, \pi/20)$ ,  $\omega_2 = (8\pi/20, \pi/20)$ ,  $\omega_3 = (15\pi/20, \pi/20)$ ,  $\omega_4 = (\pi/20, 8\pi/20)$ ,  $\omega_5 = (8\pi/20, 8\pi/20)$ ,  $\omega_6 = (15\pi/20, 8\pi/20)$ ,  $\omega_7 = (\pi/20, 15\pi/20)$ ,  $\omega_8 = (8\pi/20, 15\pi/20)$  and  $\omega_9 = (15\pi/20, 15\pi/20)$ , with respect to the regular spacing of  $7\pi/20$  (just exceeding  $\pi/3$ ). The value of  $\sigma^2$  is calculated using equation (5) as  $\sigma^2 = 16h^2/(9\rho^2) = 0.04$ . For the considered set of locations and frequencies, the degree of freedom for ‘between spatial locations’, ‘between frequencies’ and ‘residual+ interaction’ effects are  $df_L = 8$ ,  $df_F = 8$  and  $df_{IEr} = 64$ , respectively. We denote ‘between spatial locations’, ‘between frequencies’ and ‘residual+ in-

interaction' sum of squares with  $SSL$ ,  $SSF$  and  $SSIEr$ , respectively. In the analysis of variance table, we first evaluate the significance of the interaction effect. If  $SSIEr/\sigma^2 > \chi_{64}^2(0.05)$ , we conclude that the point pattern is nonstationary, and nonuniformly modulated. If the interaction is not significant, we conclude that the point pattern is a uniformly modulated process, and proceed to test for stationarity versus the zonal stationarity by comparing  $SSL/\sigma^2$  with  $\chi_8^2(0.05)$ . Significance of the location effect suggests that the point pattern is nonstationary. Similarly, to evaluate between frequencies effect,  $SSF/\sigma^2$  is compared with  $\chi_8^2(0.05)$  and the significance of test confirms that the spectra is nonuniform.

In the following study, we simulate 100 realizations from a stationary and a nonstationary point process to study the empirical size and power of the proposed test. Table 1 shows the ratios of rejections of stationarity assumption. The ratios of rejections for stationary processes represent the empirical size and the ratios of rejections for nonstationary processes represent the empirical power of the test. We consider realizations of Thomas process because of its clustered behavior which makes it similar to a zonal stationary process. To simulate a Thomas process of the parameter  $(\delta, \tau, \mu)$ , the 'parent' point process is generated at first according to a stationary Poisson point process of intensity  $\delta$  in the study region. Then, each parent point is replaced independently by 'offspring' points which the number of offspring points of each parent is generated according to a Poisson distribution with mean  $\mu$ . Finally, the position of each offspring relative to its parent location is determined by a bivariate normal distribution centered at the location of parent with covariance matrix  $diag(\tau^2, \tau^2)$ . The process is denoted by  $T(\delta, \tau, \mu)$  and is chosen because of its clustered behavior which makes it similar to a zonal stationary process. The number of observed points is an increasing function of  $\delta$  in Thomas process. We also consider the realizations of stationary Poisson processes of intensity  $\lambda$ , denoted by  $P(\lambda)$ . The results of Table 1 show that the empirical size of test decreases for the larger values of  $\delta$  and approaches the nominal level. The great values of empirical size are due to the use of asymptotic normal distribution for  $Y_{ij}$ . In fact, this asymptotic behavior is valid for large enough number of points at each grid. For different realizations of stationary Poisson processes, the empirical size is zero. For the point pattern  $y$  shown in Figure 3, the point pattern in  $\mathbf{S}_3$  is a realization of the stationary Thomas process with parameters  $\delta = 0.046$ ,  $\tau = 1$  and  $\mu = 4$ , and the point pattern in  $\mathbf{S}_8$  is a realization of the SSI process with Inhibition distance  $r = 1.5$ .

To simulate a SSI process with Inhibition distance  $r$ , points are added one-by-one. Each new point is generated according to uniform distribution in the window and is independent of previous points. If the new point lies closer than  $r$  from an existing point, then it is rejected and another random point is generated. The empirical power of test is close to one for the point pattern  $y$ . The empirical power of test is equal to one in all the nonstationary cases.

Since the value of the periodogram at higher frequencies can be taken as the contribution of random errors only, so we ignore  $\omega_9 = (15\pi/20, 15\pi/20)$  (the frequency with the highest norm) and perform the test by considering  $\omega_1, \dots, \omega_8$ . Therefore, we have  $df_F = 7$  and  $df_{IEr} = 56$ . The results of Table 1

TABLE 1  
The rejections ratios of stationarity in 100 times replications of testing procedure  
with the realization of Thomas and Poisson point processes.

Model	using 9 frequencies	without $\omega_9$
$T(2,1,6)$	0.10	0.04
$T(2,1,8)$	0.13	0.08
$T(5,0.25,4)$	0.12	0.02
$T(5,0.25,6)$	0.06	0.05
$T(5,0.25,8)$	0.06	0.03
$T(5,0.5,4)$	0.02	0.01
$T(5,0.5,6)$	0.00	0.01
$T(5,0.5,8)$	0.05	0.01
$T(5,1,4)$	0.03	0.02
$T(5,1,6)$	0.00	0.00
$T(5,1,8)$	0.00	0.00
$T(7,0.25,4)$	0.06	0.02
$T(7,0.25,6)$	0.02	0.00
$T(7,0.25,8)$	0.04	0.02
$T(7,0.5,4)$	0.01	0.00
$T(7,0.5,6)$	0.02	0.01
$T(7,0.5,8)$	0.00	0.00
$T(7,1,4)$	0.00	0.00
$T(7,1,6)$	0.00	0.00
$T(7,1,8)$	0.00	0.00
$P(20)$	0.00	0.00
$P(30)$	0.00	0.00
$P(50)$	0.00	0.00
$P(0.1 \exp(0.2 \sin(4\pi x) + 0.1y))$	1.00	1.00
$T(3, 0.2, \exp(3 \sin(4\pi xy) + 0.01x))$	1.00	1.00
$y$	0.98	1.00

show that the empirical size of test decreases when  $\omega_9$  is removed from the set of considered frequencies.

#### 4.1. Real data

##### 4.1.1. Trees data

As mentioned earlier, the first dataset is devoted to the locations of *Euphorbiaceae* trees, as shown in Figure 1. Postulating that all of the assumptions made in Section 4 are valid for this case, we consider  $h = 3$  and  $\rho = 34$ . Thus, the distance between the locations  $z_i$  and frequencies  $\omega_j$  points must be at least  $\rho = 34$  and  $\pi/h = \pi/3$ , respectively, and the value of  $\sigma^2$  will be equal to  $\sigma^2 = 16h^2/(9\rho^2) = 0.0138$ . The points  $z_1, \dots, z_4$  are the centroids of the four equally- dimensioned subregions denoted by  $\mathbf{S}_1, \dots, \mathbf{S}_4$  from left to right and down to up, respectively. In other words, the points  $z_i$  are chosen as  $z_1 = (70/4, 70/4)$ ,  $z_2 = (3 \times 70/4, 70/4)$ ,  $z_3 = (70/4, 3 \times 70/4)$ , and  $z_4 = (3 \times 70/4, 3 \times 70/4)$ . We denote the restricted point patterns to  $\mathbf{S}_1, \dots, \mathbf{S}_4$  by  $\mathbf{x}_1, \dots, \mathbf{x}_4$ , respectively. The number of observed trees at the regions  $\mathbf{S}_1, \dots, \mathbf{S}_4$  are almost the same. Firstly, we consider the estimate of  $K$  function for investigating the inter-point dependence aspects of these point patterns. The sample  $K$  functions of each point pattern along the theoretic  $K$  function of the stationary Poisson process are shown in Figure 6. Simply speaking, the gray areas of all the figures represent the acceptance regions of the stationary Poisson model

for data. The hypothesis of stationary Poisson model is rejected based on a statistic at level of  $\alpha = 0.05$ , when the sample statistic does not remain between the given boundaries at least for a point  $r \in \mathbb{R}_+$ . When the sample  $K$  functions compared with the prepared boundaries, the lack of fitness of stationary Poisson process to all of the point patterns is emphasized. Visually, the sample  $K$  functions of all the point patterns expect  $\mathbf{x}_2$  are approximately the same. In the following, we apply our proposed method to test the nonstationarity of this point pattern. Afterwards, if the test rejects the stationarity assumption against the zonal stationarity, then we use the post-hoc tests for detecting the location(s) at which the structure of trees pattern is changed.

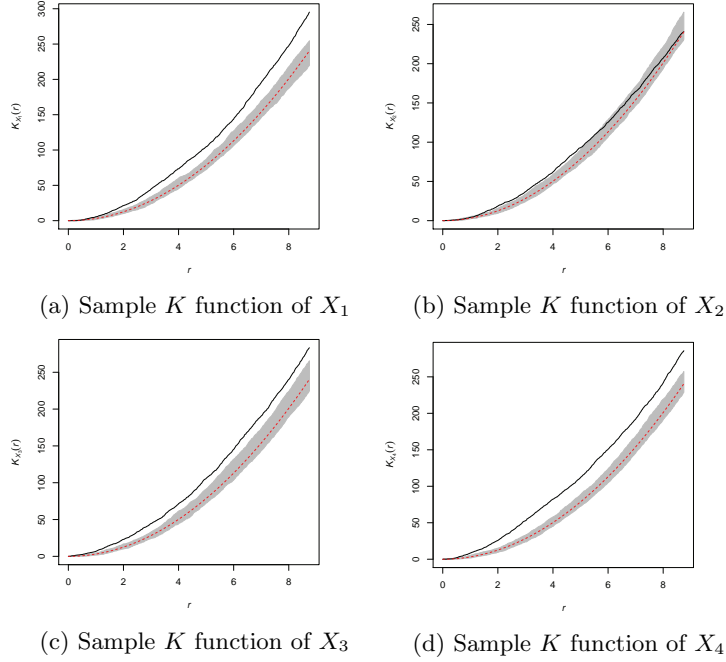


Fig 6: The estimated  $K$  function for trees data computed for point patterns restricted in square windows with centers  $z_1, \dots, z_4$  and the resulting point process is mentioned by  $X_1, \dots, X_4$ , respectively. The figures contain the sample  $K$  functions (solid line), the theoretic functions for the stationary Poisson point process (dashed red line), and upper and lower boundaries based on the enveloping of 99 simulations from stationary Poisson process (gray area).

Table 2 shows the results of post-hoc test. There is a significant difference between the local periodograms at locations  $z_2$  and  $z_4$ , while the behavior of the local periodograms dose not change at other locations. Since the number of observed trees in both areas ( $\mathbf{S}_2$  and  $\mathbf{S}_4$ ) is almost the same, so the difference between the local periodograms at locations  $z_2$  and  $z_4$  may be due to the significance of the latitude effect on the competition between trees.

TABLE 2  
The Bonferroni post-hoc test for the trees data.

Item	Df	$\chi^2(= SS/\sigma^2)$ statistic	p-value
$z_1$ vs $z_2$	1	1.38	0.24
$z_1$ vs $z_3$	1	0.12	0.73
$z_1$ vs $z_4$	1	4.99	0.03
$z_2$ vs $z_3$	1	0.69	0.41
$z_2$ vs $z_4$	1	11.64	$< 0.05/6 = 0.008^*$
$z_3$ vs $z_4$	1	6.66	0.01

Table 3 presents the results of the analysis of variance for this setting of locations and frequencies using the logarithm of local periodogram. The interaction term is not significant ( $\chi^2$  is small compared to  $\chi_{24}^2(0.05) = 36.42$ ) confirming that the point pattern is uniformly modulated. Moreover, both ‘between spatial locations’ and ‘between frequencies’ sums of squares are highly significant ( $SSL/\sigma^2 > \chi_3^2(0.05) = 7.81$  and  $SSF/\sigma^2 > \chi_8^2(0.05) = 15.51$ ), suggesting that the point pattern is nonstationary and that the spectra are nonuniform. The analysis of variance indicates a significant difference in the locations effect. Thus, we use the Bonferroni method for multiple comparisons to discover different locations. There is a set of  $\binom{4}{2} = 6$  hypotheses to test, say,  $\alpha_i = \alpha_j$  for  $i \neq j$  and  $i, j = 1, \dots, 4$ . The Bonferroni method rejects each test if  $SSL/\sigma^2 > \chi_1^2(\alpha/6)$ . The Bonferroni method simply reduces the significance level of each individual test so that the sum of the significance levels is no greater than  $\alpha$ .

TABLE 3  
Analysis of variance table for the trees data.

Item	Df	SS	$\chi^2(= SS/\sigma^2)$
Between spatial locations	3	0.18	12.74
Between frequencies	8	11.60	838.00
Interaction + residual	24	0.37	26.60
Total	35	12.14	877.34

#### 4.1.2. Capillaries data

The stationary Strauss hard-core model was suggested for the locations of capillaries in prostate tissues [11, 12]. It has been concluded that capillary profile patterns are more clustered in healthy tissue than in cancerous tissue the difference in the spatial model of healthy and cancerous tissues was verified [8] by testing the corresponding empirical  $K$  functions. The intensities of two point patterns are almost the same. According to the stationarity assumption considered by [11, 12] to these patterns, the second order properties of healthy and cancerous tissues were compared [20] and concluded that cancer does not affect the first and second order properties of the locations of capillaries on the prostate tissue. All these researches assumed the corresponding point process to be stationary. Here, we apply our proposed method to test the nonstationarity

of both point patterns. The observation windows are rescaled to  $[0, 70]^2$  cubes and all the required values are assumed to be same as the the previous settings.

TABLE 4  
*Analysis of variance table for the Capillaries data.*

Healthy tissue			
source of variation	$df$	$SS$	$\chi^2(=SS/\sigma^2)$
Between spatial locations	3	0.21	15.00
Between frequencies	8	2.77	200.03
Interaction + residual	24	0.39	27.84
Total	35	3.36	242.87
Cancerous tissue			
source of variation	$df$	$SS$	$\chi^2(=SS/\sigma^2)$
Between spatial locations	3	0.53	38.20
Between frequencies	8	1.90	136.94
Interaction + residual	24	0.25	17.96
Total	35	2.67	193.09

TABLE 5  
*The Bonferroni post-hoc test for the Capillaries data. The significant differences in the location effects are denoted by ‘\*’.*

Healthy tissue			
test	$df$	$\chi^2 = SS/\sigma^2$	$p$ -value
$z_1$ vs $z_2$	1	4.65	0.03
$z_1$ vs $z_3$	1	13.94	$< 0.05/6 = 0.008^*$
$z_1$ vs $z_4$	1	7.60	0.006*
$z_2$ vs $z_3$	1	2.49	0.11
$z_2$ vs $z_4$	1	0.36	0.55
$z_3$ vs $z_4$	1	0.95	0.33
Cancerous tissue			
test	$df$	$\chi^2 = SS/\sigma^2$	$p$ -value
$z_1$ vs $z_2$	1	18.53	$< 0.05/6 = 0.008^*$
$z_1$ vs $z_3$	1	32.45	$< 0.008^*$
$z_1$ vs $z_4$	1	22.35	$< 0.008^*$
$z_2$ vs $z_3$	1	1.94	0.16
$z_2$ vs $z_4$	1	0.18	0.67
$z_3$ vs $z_4$	1	0.94	0.33

The results of the analysis of variance and post-hoc test for this dataset are presented at Table 4 and 5, respectively. The results show that the location effect is significant for both of the healthy and cancerous point patterns. According to the new obtained evidence, the previous results could not be invoked. Nevertheless, we can use the local periodograms to extend the idea of [20] for comparing the spectral density functions of nonstationary point patterns. The asymptotic independence and the asymptotic distribution of local periodograms are used to compute the density function of the local periodograms and hence the likelihood function in terms of the local periodograms similar to [20]. Let  $I_{z_i}^h(\omega_j)$  denotes to the local periodogram of healthy point pattern at the location

$z_i$  and frequency  $\omega_j$  and there is similar notation, i.e.,  $I_{z_i}^c(\omega_j)$ , for cancerous one. Thus, the likelihood ratio for comparing the local spectral density functions of two independent point patterns at the location  $z_i$  will be as below.

$$\Lambda_{z_i} = \prod_{j=1}^9 \frac{4I_{z_i}^h(\omega_j)I_{z_i}^c(\omega_j)}{(I_{z_i}^h(\omega_j) + I_{z_i}^c(\omega_j))^2}$$

Finally, the resulting likelihood ratio is compared with 0.025 and 0.975 quintiles estimated using the simple Monte Carlo simulation. The values of  $\Lambda_{z_i}, i = 1, \dots, 4$  are 0.93, 0.95, 0.89 and 0.94, respectively, and the estimated quintiles are  $1.07 \times 10^{-5}$  and 0.20. The results of likelihood ratio test show that there are significant difference between the local spectral density functions of healthy and cancerous point patterns at the locations  $z_i, i = 1, \dots, 4$ . Therefore, assuming the nonstationarity of both point patterns, we can conclude that cancer affects the second order structure of prostate tissue.

## References

- [1] BANDYOPADHYAY, S. and RAO, S. S. (2016). A test for stationarity for irregularly spaced spatial data. *Journal of the Royal Statistical Society: Series B (Statistical Methodology)*.
- [2] BARTLETT, M. S. (1964). The spectral analysis of two-dimensional point processes. *Biometrika* **51** 299–311. [MR0175254](#)
- [3] CORSTANJE, R., GRUNWALD, S. and LARK, R. (2008). Inferences from fluctuations in the local variogram about the assumption of stationarity in the variance. *Geoderma* **143** 123–132.
- [4] DAHLHAUS, R. (1996). Asymptotic statistical inference for nonstationary processes with evolutionary spectra. In *Athens Conference on Applied Probability and Time Series Analysis, Vol. II (1995). Lecture Notes in Statist.* **115** 145–159. Springer, New York. [MR1466743](#)
- [5] FUENTES, M. (2002). Modeling and prediction of nonstationary spatial processes. *Statistical Modeling* **9** 281–298.
- [6] FUENTES, M. (2005). A formal test for nonstationarity of spatial stochastic processes. *J. Multivariate Anal.* **96** 30–54. [MR2202399](#)
- [7] GUYON, X. (1982). Parameter estimation for a stationary process on a  $d$ -dimensional lattice. *Biometrika* **69** 95–105. [MR655674](#)
- [8] HAHN, U. (2012). A studentized permutation test for the comparison of spatial point patterns. *Journal of the American Statistical Association* **107** 754–764.
- [9] JENKINS, G. M. (1961). General considerations in the analysis of spectra. *Technometrics* **3** 133–166. [MR0125731](#)
- [10] JUN, M. and GENTON, M. G. (2012). A test for stationarity of spatio-temporal random fields on planar and spherical domains. *Statist. Sinica* **22** 1737–1764. [MR3027105](#)



- [11] MATTFELDT, T., ECKEL, S., FLEISCHER, F. and SCHMIDT, V. (2006). Statistical analysis of reduced pair correlation functions of capillaries in the prostate gland. *Journal of microscopy* **223** 107–119.
- [12] MATTFELDT, T., ECKEL, S., FLEISCHER, F. and SCHMIDT, V. (2007). Statistical modelling of the geometry of planar sections of prostatic capillaries on the basis of stationary Strauss hard-core processes. *Journal of microscopy* **228** 272–281.
- [13] MONDAL, D. and PERCIVAL, D. B. (2012). Wavelet variance analysis for random fields on a regular lattice. *IEEE Trans. Image Process.* **21** 537–549. [MR2920639](#)
- [14] MUGGLESTONE, M. A. and RENSHAW, E. (1996). A practical guide to the spectral analysis of spatial point processes. *Comput. Statist. Data Anal.* **21** 43–65. [MR1380832](#)
- [15] PRIESTLEY, M. (1967). Power spectral analysis of non-stationary random processes. *Journal of Sound and Vibration* **6** 86–97.
- [16] PRIESTLEY, M. B. (1965). Evolutionary spectra and non-stationary processes.(With discussion). *J. Roy. Statist. Soc. Ser. B* **27** 204–237. [MR0199886](#)
- [17] PRIESTLEY, M. B. (1966). Design relations for non-stationary processes. *J. Roy. Statist. Soc. Ser. B* **28** 228–240. [MR0199943](#)
- [18] PRIESTLEY, M. B. and SUBBA RAO, T. (1969). A test for non-stationarity of time-series. *J. Roy. Statist. Soc. Ser. B* **31** 140–149. [MR0269062](#)
- [19] RENSHAW, E. and FORD, E. D. (1983). The Interpretation of Process from Pattern Using Two-Dimensional Spectral Analysis: Methods and Problems of Interpretation. *J. Roy. Statist. Soc. Ser. B.* **32** 51-63.
- [20] SAADATJOUY, A. and TAHERIYOUN, A. (2016). Comparing the second-order properties of spatial point processes. *Statistics And Its Interface* **9** 365–374.

Department of Statistics,  
Shahid Beheshti University, G.C.  
Evin, 1983969411, Tehran, Iran.  
e-mail: [a\\_saadatjouy@sbu.ac.ir](mailto:a_saadatjouy@sbu.ac.ir)

Department of Statistics,  
Shahid Beheshti University, G.C.  
Evin, 1983969411, Tehran, Iran.  
e-mail: [a\\_taheriyoun@sbu.ac.ir](mailto:a_taheriyoun@sbu.ac.ir)

Department of Statistics,  
Shahid Beheshti University, G.C.  
Evin, 1983969411, Tehran, Iran.  
e-mail: [m-vahidi@sbu.ac.ir](mailto:m-vahidi@sbu.ac.ir)